Geobios xxx (xxxx) xxx

Contents lists available at ScienceDirect

Geobios

journal homepage: www.elsevier.com/locate/geobio

Research Paper

First evidence of ichnopathologies in *Rhinoceripeda tasnadyi* tracks from the Miocene of Hungary

M. Belvedere [a,*], F. Bertozzo [b,c], G. Botfalvai [d,e], L. Pandolfi [f]

[a] Dipartimento di Scienze della Terra, Università di Firenze, Via G. La Pira, 50121, Firenze, Italy
[b] Operational Directorate Earth and History of Life, Royal Belgian Institute of Natural Sciences, Brussels, Belgium
[c] CI2Paleo, Sociedade de Historia Natural, Travessa Florêncio Augusto Chagas n°8B, R/C, 2560-230 Torres Vedras, Portugal
[d] Institute of Geography and Earth Sciences, Department of Paleontology, Eötvös Loránd University, Budapest, Hungary
[e] HUN-REN-MTM-ELTE Research Group for Paleontology, H-1431 Budapest, P.O. Box 137, Hungary
[f] Dipartimento di Scienze della Terra, Università di Pisa, Via S. Maria 53, 56126, Pisa, Italy

ARTICLE INFO

Article history:
Received 28 November 2023
Revised 21 July 2024
Accepted 5 August 2024
Available online xxxx

Keywords:
Rhinoceripeda tasnadyi
Rhino
Paleopathology
Vertebrate ichnology
Miocene
Hungary

ABSTRACT

Despite a vast record, ichnological evidence of malformed or injured animals is extremely rare. During the re-examination of slabs collected from the Ipolytarnóc tracksite (Early Miocene, North Hungary) and housed at the Supervisory Authority for Regulatory Affairs, three "atypical" tracks were detected along the same trackway. They belong to the ichnotaxon *Rhinoceripeda tasnadyi*, attributed to a medium- to large-sized "hornless" Miocene rhinocerotids. The hoof of the left digit III appears to be split, rather than oval, at approximatively half of its width, giving an almost tetradactyl appearance to the footprints. The deformation due to overprinting is excluded because of the number of tracks showing the same variation. This injury/malformation could be identified as the atypical tracks belong to a trackway where the opposite impression is preserved and due to the large number of accessible *R. tasnadyi* footprints. These account for a wide range of the standard variability of the morphology at Ipolytarnóc. If the track record was limited, or when the atypical tracks do not belong to a trackway, it would not be possible to recognise those differences as ichnopathologies and, as a result, a different trackmaker would have been assessed, or a wrong ichnotaxonomical diagnosis would have been attributed.

1. Introduction

The Ipolytarnóc Fossil Nature Conservation Area (hereafter named Ipolytarnóc locality) is one of the most diverse and important Neogene fossil track sites in Europe, with more than three thousand vertebrate footprints belonging to at least eleven ichnospecies described from this locality (Böckh, 1902; Tasnádi Kubacska, 1976; Kordos, 1985; Botfalvai et al., 2022). The discovery of the Ipolytarnóc trackway site dates to 1900, when Hugó Böckh went to Ipolytarnóc to study a giant silicified tree trunk and found several vertebrate footprints on the underlaying sandstone bed (Böckh, 1902). After the first discoveries, on several occasions large slabs were cut and removed from the original footprint bearing sandstone beds of Ipolytarnóc locality, which were transported to Budapest and exhibited in different Hungarian museums (Kordos, 1985). One of these removed slabs, now housed and exhibited in the Auditorium of the Geological Institute (current official name: Supervisory Authority for Regulatory Affairs), Budapest, Hungary, is investigated in this study. This 270 × 250 cm slab was excavated by T. Szontagh (Hungarian Geological Institute) in the beginning of the 1900s, but unfortunately it was removed from its original place without detailed documentation, thus its original location and orientation cannot be determined (Tasnádi Kubacska, 1976).

The first large-scale excavation of the footprintbearing sandstone beds was conducted in 1937 at the Ipolytarnóc site under the leadership of A. Tasnádi Kubacska (from the Hungarian Natural History Museum), as a result of which hundreds of vertebrate footprints were discovered and published later (Tasnádi Kubacska, 1976; Kordos, 1985; Botfalvai et al., 2022). Vialov (1965) introduced the new ichnogenus *Rhinoceripeda* and classified the Ipolytarnóc large perissodactyl tracks as the new ichnospecies *Rhinoceripeda tasnadyi*; the ichnotaxonomical analysis was completed and emended by Kordos (1985) who validated the *Rhinoceripeda tasnadyi* ichnotaxon, defining as holotype one of the trackway housed now at the Supervisory Authority for Regulatory Affairs.

☆ Corresponding editor: Vicente D. Crespo.
* Corresponding author.
E-mail address: matteo.belvedere@unifi.it (M. Belvedere).

https://doi.org/10.1016/j.geobios.2024.08.009
0016-6995/

Please cite this article as: M. Belvedere, F. Bertozzo, G. Botfalvai et al., First evidence of ichnopathologies in *Rhinoceripeda tasnadyi* tracks from the Miocene of Hungary, Geobios, https://doi.org/10.1016/j.geobios.2024.08.009

In February 2023 the material from Ipolytarnóc was re-examined; this study focusses on the slab exposed in the Auditorium of the former Geological Institute (i.e., specimen Ob.1512), now Supervisory Authority for Regulatory Affairs (SZTFH), already illustrated in Kordos (1985: p. 351, fig. 53), where some probable malformation is noticed in one of the *R. tasnadyi* trackways. A detailed description of the tracks and of the malformation is presented, together with their possible causes. It also represents the first ichnological record of malformations for fossil rhinocerotids, and one of the few already described for mammals (Oliva and Arregui, 2018).

2. Geological and geographical context

The Ipolytarnóc tracksite is located in the North Hungarian zone of the Carpathian Basin (48°14′12″ N; 19°39′25″ E), near the Slovak-Hungarian border (Fig. 1). The exposed sedimentary sequence represents the classic Lower Miocene succession of Hungary including shallow marine (Pétervására Sandstone Fm.), fluvio-lacustrine (Zagyvapálfalva Fm.) and volcanic (Tihamér Rhyolite Lapilli Tuff Fm.) sediments (Fig. 1). Although the chronostratigraphic framework of the area is based on the Central Paratethys nomenclature (such as Eggenburgian, Ottnangian and Karpatian steges; Rögl, 1998; Piller et al., 2007), these formations all represent sediments of the Burdigalian stage (Piller et al., 2007). Results of detailed geological and stratigraphical investigations of the Ipolytarnóc area have already been published in several publications (Bartkó, 1985; Harangi, 2001; Pálfy et al., 2007; Karátson et al., 2022). Therefore, in this section of the present paper only a brief overview is given of the main characteristics of the geological background of this area.

The oldest fossil-rich sediments exposed in the Ipolytarnóc area is the glauconitic sandstone of the nearshore facies of the Pétervására Sandstone Fm. (Sztanó, 1994), from where unusually diverse and abundant marine Eggenburgian mollusc fauna and shark teeth assemblages were discovered (Csepreghyné, 1967; Kocsis, 2007). This shallow marine sandstone is covered by the terrestrial succession of the Zagyvapálfalva Fm. consisting of variegated siltstone, conglomerates, and sandstones. The fluvial-floodplain sediments of the Zagyvapálfalva Fm. are, in the Ipolytarnóc area, 8–10 m thick; the investigated tracks are found in the latest 40 cm (Bratkó, 1985). The footprint-bearing beds of Ipolytarnóc consist of alternating thick and thin lamination of the clayish and silty sandstone beds. A detailed sedimentological investigation and review of the footprint bearing sandstone layers is currently in progress; preliminary data identified tracks at least in the uppermost two horizons of the succession (Botfalvai et al., 2022). The occasional dense plant cover around the river channel indicates frequent flooding and seasonal water oscillation in a subtropical rainforest environment (Hably, 1985). The footprint bearing succession of Zagyvapálfalva Fm. is covered by a 20–40 m-thick rhyolite lapilli tuff, more recently called the Tihamér Riolite Lapilli Tuff Fm. (Lukács et al., 2022). This Lapilli Tuff fm. (former name of this formation was Gyulakeszi Rhyolite Tuff Fm.) directly covers

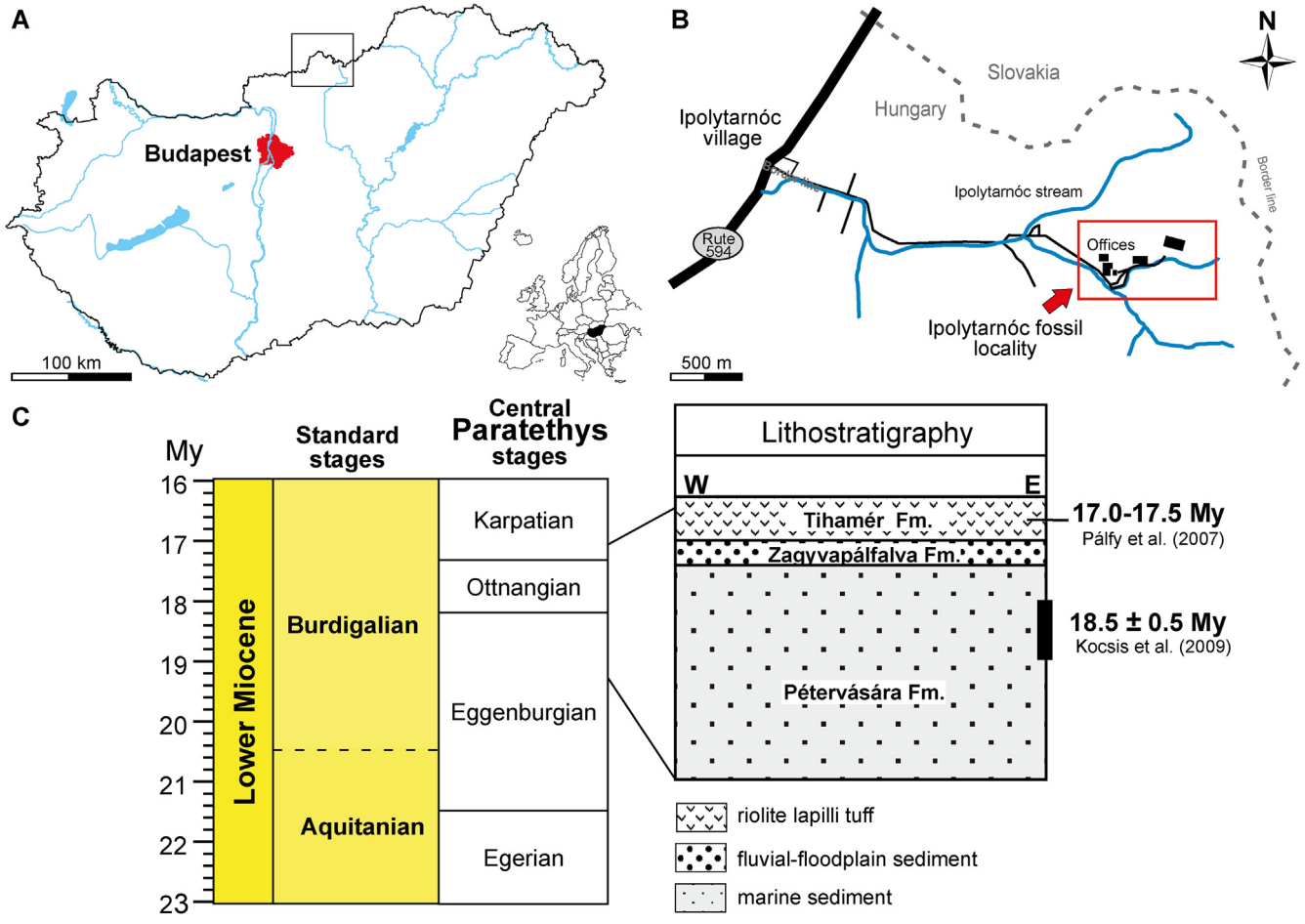

Fig. 1. Geographic and geological position of the investigated area. **A, B.** Position of Ipolytarnóc locality near the Slovakian-Hungarian border. **C.** Stratigraphic position of the Lower Miocene formations at Ipolytarnóc locality (based on Gradstein et al., 2012; Kocsis, 2007; Kocsis et al., 2009; Pálfy et al., 2007).

the underlying footprint horizons, thus the radiometric ages measured from the tuff can be used to constrain the age of the footprint horizon as well (Pálfy et al., 2007; Karátson et al., 2022). The radiometric measurements (Pálfy et al., 2007; Karátson et al., 2022; Lukács et al., 2021, 2022) and palaeomagnetic studies (Márton et al., 2007) of the rhyolite tuff exposed at Ipolytarnóc locality indicate an approximate age of 17.0–17.5 Ma correlating with the MN4 Mammal zone; this age is also interpreted as the date of the Ipolytarnóc trace fossils.

3. Material and methods

3.1. Labelling and measures

Trackways were named "Rh" for *Rhinoceripeda* followed by the trackway number, given following the occurrence in the slab, from left to right. The numbering within the trackways was made in relation to the sagittal orientation of the limb which left the imprint: L for left and R for right, P for pes (foot) and M for manus (hand) impressions. Following Paratte et al. (2018) all trackways ideally begin with a left pes and manus (LP1 and LM1), followed by the right pes/manus (RP1 and RM1); where the first left prints are not present, the trackway begins with RP1/RM1, followed by LP2/LM2 (i.e., LP1/LM1 are missing from that trackway). Isolated tracks where all labelled RhI as for *Rhinoceripeda* isolated, followed by a number.

All measurements (Fig. 2) were taken from the 3D models (see below) with CorelDraw. The following abbreviations are used: PL: Pes Length; PW: Pes Width; dII, dIII, dIV: digit II, III and IV, respectively; pIIL, mIIL, pIIIL, mIIIL, pIVL, mIVL: length of pes (p) and manus (m) digit II, III and IV, respectively; pIIW, mIIW, pIIIW, mIIIW, pIVW, mIVW: width of pes (p) and manus (m) digit II, III and IV, respectively; P: Pace Length; S: Stride Length; PA: Pace Angulation. All measures are reported in Table S1 (Appendix A). A corelation with Kordos' (1985: p. 351, fig. 53) labelling is given in Table S1 (Appendix A); tentative correlations are marked with a "?".

3.2. 3D models

Close-range photogrammetric models were generated for all the tracks and the trackways analysed here. The photos were taken

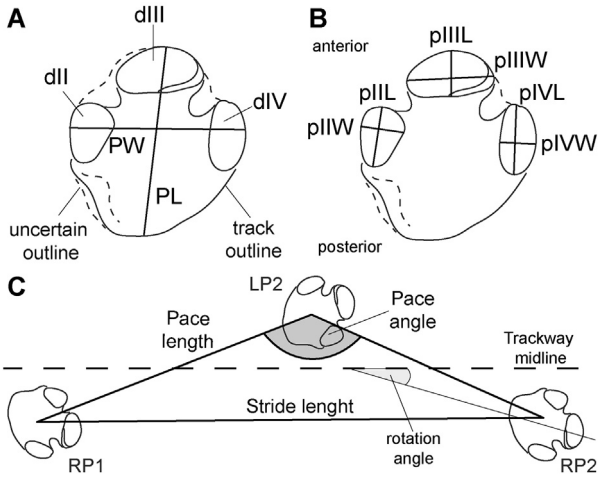

Fig. 2. Measurements. The track used as reference is the neotype of *Rhinoceripeda tasnadyi* (Kordos, 1985) redrawn by the authors. **A.** Perissodactyl pes track (right). Track length (PL) and width (PW), labelling of digits and explanation of the lines used. **B.** Perissodactyl digit measures. Digit II length and width (pIIL, pIIW), digit III length and width (pIIIL, pIIIW), digit IV length and width (pIVL, pIVW). **C.** Trackway parameters.

with a 20.4 MPixel Canon EOS 70D camera, equipped with a Canon STL 10–18 mm lens and a ring flash. The processing of photos for 3D photogrammetry was done with Agisoft Metashape (v.1.8.4, https://www.agisoft.com), following the guidelines available (Lallensack et al., 2022; Mallison and Wings, 2014; Matthews et al., 2016). 686 photos were used to generate a 70-million-polygon mesh that was then exported in Stanford PLY format, without texture but with RGB values integrated (Falkingham et al., 2018). The PLYs were processed with the freeware CloudCompare (https://www.cloudcomapre.com) for a more accurate orientation and to generate depth-maps and contour lines (Lallensack et al., 2022). The 3D models and their metadata are available to download on MorphoSource (specimen V 2024.9.1: https://doi.org/10.17602/M2/M632895; specimen Ob.1512: https://doi.org/10.17602/M2/M633401), as in the best practice indicated in Falkingham et al. (2018). The 3D models are registered within the Department of Collections of the Supervisory Authority for Regulatory Affairs (SZTFH) in digital form, with the IDs V 2024.9.1 and Ob.1512 for the Auditorium slabs. Redistribution, sublicensing or transfer of the 3D models and data is prohibited (for instance, they cannot be made available for download on websites) without a separate and prior written permission from the SZTFH, as are the 3D prints or other replicas derived from the models.

4. Results

Forty-one rhinocerotid tracks (against the 39 of Kordos, 1985) and 5 trackways were identified, together with several artiodactyl tracks, not included in this study (Fig. 3). Most of the tracks on the surface are well preserved, with a morphological preservation grade of 2 (Marchetti et al., 2019), even though some less well preserved, or fainter (grade 1) tracks occur as well. In some parts of the slab, there is a heavy overprinting of rhinocerotid tracks that sometimes makes difficult to identify the trackway sequence. No unequivocal manus tracks have been found, and therefore they are described all as pes; there are, however, three cases (RhI3 as possible Rh1-RM2; RhI17 as possible Rh4-RM1; RhI20 as possible Rh4-RM2) where the track could be a manus impression (Fig. 3), but we preferred to consider the possible manus as isolated tracks. This uncertainty is given by the similar morphology of the pes and manus, which are not distinguishable unless when arranged in a trackway.

We agree with the ichnotaxonomical attribution of these tracks to *Rhinoceripeda tasnadyi* made by Kordos (1985), as they significantly differ from the *Rhinoceripeda voconcense*, the only other species of this ichnogenus (Belvedere et al., 2023); the difference with this ichnotaxon are in the sole region, that *in R. tasnadyi* is always rounded, while in *R. voconcense* is generally subcircular for the pes and trapezoidal for the manus (Belvedere et al., 2023).

No information on the original orientation of the slab is available, therefore the trackways direction is determined from the exposition; mostly all the trackways and most of the tracks go from the top to the bottom of the slab, and only four seem to be oriented towards the top of the slab (Fig. 3). We describe here in detail the morphology of the "atypical" tracks (Rh3), while we provide only the general description for the shape of the "normal" tracks.

4.1. General track description

Tracks are as wide as long (average PW/PL: 1.01), with an average PL of 190 mm and PW of 192 mm (Table S1; Appendix A). They are always tridactyl. The heel impression is not always visible, but when present it has a subcircular shape. The impressions of digits II, III and IV are often well marked. Digit III has the largest

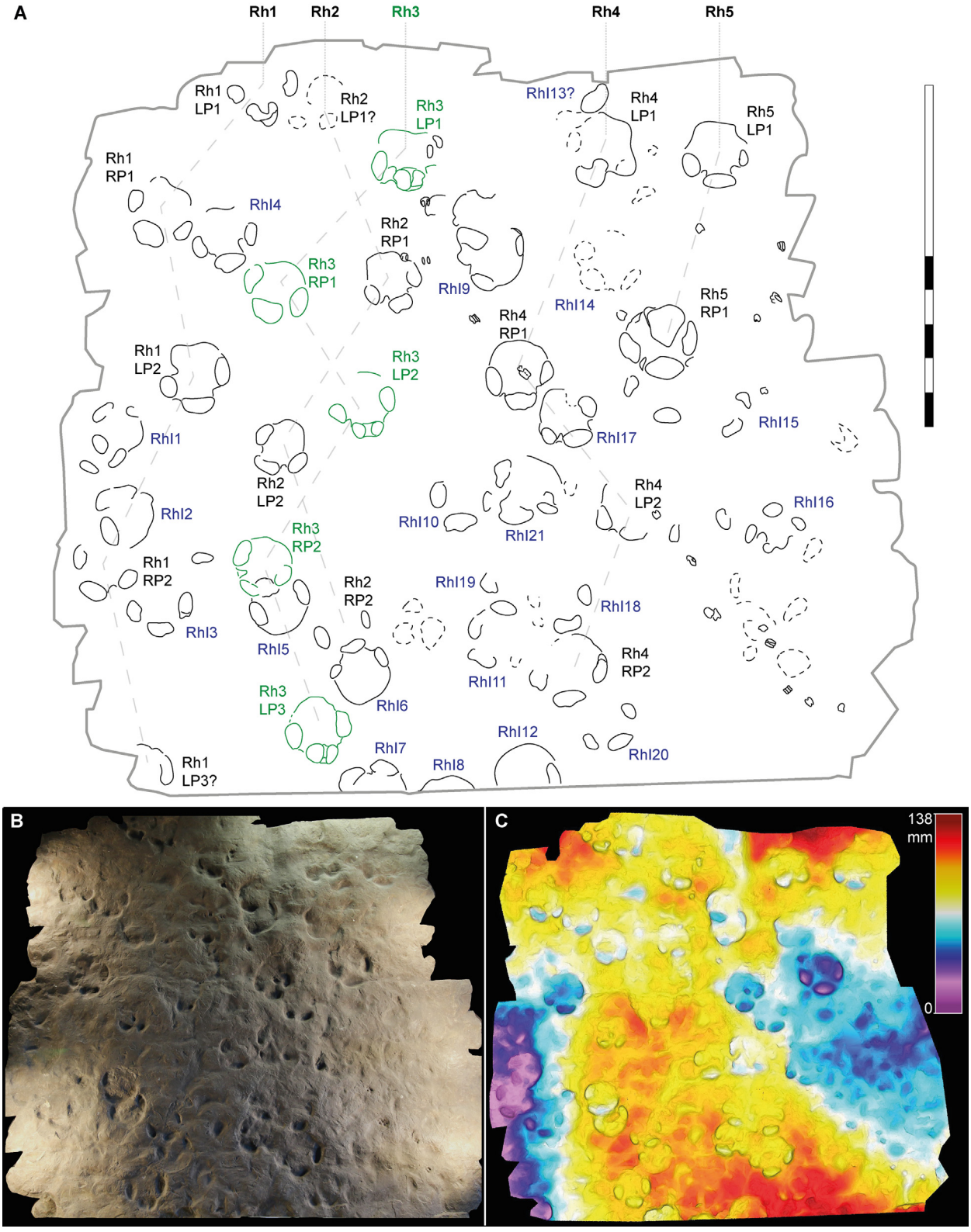

Fig. 3. The slab Ob.1512 exposed in the SZTFH Auditorium. **A.** Schematic outline drawings on the slab made from the 3D model. The green lines highlight trackway Rh3, object of this study. Dashed grey lines indicate trackway interpretation; black track labels are for prints arranged in trackway; blue labels are for isolated tracks. **B.** Photograph of the slab in the Auditorium. **C.** False-colour depth map derived from the photogrammetric 3D model. Since the surface is quite uneven, the colour scale indicates only the max difference between the lowest (dark purple) and highest (dark red) points. Scale bar: 1 m (A). (For interpretation of the references to colour in this figure legend, the reader is referred to the web version of this article.)

impression, larger than long (pIIIL: 51 mm; pIIIW: 86 mm). Digits II and IV impressions are longer than wide, oval, subparallel, and slightly converging anteriorly, with digit II always smaller than digit IV (pIIL: 65 mm, pIIW: 40 mm; pIVL: 74 mm, pIVW: 40 mm). The oval-shaped digit III is wider than long (pIIIL: 36 mm, pIIIW: 59 mm); it is the most marked (deepest) digit

impression. Pes tracks axis is rotated on average 15° outward with respect to the trackway mid-lines.

4.2. Trackway Rh3

It is a continuous trackway composed of 5 pes tracks (Figs. 3, 4(A)). All tracks but Rh3-LP1, which misses dIV, are very well preserved (grade 2). The track morphology is very consistent with all the other tracks of the site, being only very slightly wider than long (PW/PL: 1.03), and having digit III the largest, followed by digit IV and II. The pace length ranges from 440 mm to 545 mm, with a pace angle constant at 120°. All tracks are outward rotated by an angle ranging from 11° to 13°.

What is unusual in this trackway is the systematic occurrence on all left prints of an anomalous digit III. The digit III impressions show an atypical splitting within the impression producing a peculiar internal morphology with two deeper lobes separated by a narrow, more relieved part (normal track: Fig. 4(B); atypical track: Fig. 4(C–E)). The lobes are sub-oval in shape, although some size differences occur, with the one on the internal side always slightly bigger than the other one. When compared with the right tracks of Rh3, the left tracks have the same overall shape typical of *R. tasnadyi* (Fig. 4(F)), with the only difference of digit III. No clear difference in pace lengths, stride lengths or track rotation in relation to the trackway midline occur in Rh3 (Table S1; Appendix A), showing, at least in the short segment of the trackway preserved, no limping gait. So far, this unique feature of digit III has not been recorded in any of the right tracks of Rh3, nor in any other tracks from the thousands from the Ipolytarnóc tracksite.

5. Discussion

As a track is the result of the combination of sedimentology, locomotion and anatomy of the trackmaker (Falkingham, 2014), these three factors were considered to explain the atypical shape of Rh3 left digit III impressions. A sedimentological cause (e.g., different water content in the sediment, or different rheological properties of the sediment) is excluded because there is no difference in morphological preservation (Marchetti et al., 2019) between the right and left side of the trackway in terms of shape, but also depth of the tracks. As additional support, tracks of other animals impressed in proximity of the atypical ones do no show the same atypical digit III impression. Locomotion can be excluded as cause of the digit III impression morphology: the pace lengths are similar between left and right side, implying a similar movement of the limbs – the atypical morphology would be expected to be symmetrical and occur on both sides of the trackway, and not just in the left one. Therefore, the only explanation left is the anatomy of the trackmaker. In this regard, the asymmetry of the tracks is interpreted as result of a deformation derived by malformation or injuries. It represents a unique case in the published rhinocerotid track record, including both modern and fossil tracks, and one of the few ichnopathologies documented in the paleontological record.

5.1. Ichnopathologies in the fossil record

The ichnological record of pathologies is quite scarce and mostly focussed on the dinosaur tracks (few researches have been conducted on anomalous dinosaur tracks and less recognised these anomalies as paleopathologies; Oliva and Arregui, 2018). This is surely due to the difficulties, in the fossil record, to discriminate between a pathology or a peculiar morphology, related to substrate/locomotion interference with the track morphology, or the actual peculiar shape of the autopodium (McCrea et al., 2015). As a result, all ichnopathologies identified in the fossil record can be ascribed to three categories: (*i*) those identified for a clear difference between the left and right tracks left by the same individual (Ishigaki and Lockley, 2010; Avanzini et al., 2008; McCrea et al., 2014, 2015; Oliva and Arregui, 2018); (*ii*) those identified by an asymmetry in the pace length (Dantas et al., 1994; Ishigaki and Lockley, 2010); and (*iii*) those identified by a combination of (*i*) and (*ii*) (Ishigaki and Lockley, 2010). With the exception of cases like the one in McCrea et al. (2015: fig. 12), identifying ichnopathologies from a single footprint is virtually impossible. The even scarcer evidence from the mammalian ichnological record is probably due to the reduced ichnological studies (compared to dinosaurs'), but also to the different morphology of the tracks. However, having the possibility to check on pathologies of animal closely relative to those of the fossil record could allow deeper understanding on how a pathology is recorded by the ichnological record, and more studies on modern animals should be carried out.

5.2. A comparison with pathologies in modern rhinos and paleopathologies in the fossil record

Rhinocerotidae has a long history of pathological (Regnault et al., 2013) and paleopathological analyses (Stilson et al., 2016) supported by the general interest on this clade and an extensive fossil record. In particular, foot diseases and abnormalities have been studied extensively because of their potential implications on a modern population's welfare, even though the clinical treatment (following a potential diagnosis) can be dangerous for the animal itself (Regnault et al., 2013). To study the possible presence of diseases in these animals, in fact, they need to be sedated or anaesthetised, requiring profound clinical justification (Galateanu et al., 2013). Generally, in ungulates, compound fractures can be usually found in metacarpals and metatarsals because of limited amount of soft tissue supporting the bones (Kanniappan and Gopinadhan, 2024). In rhinocerotids, soft tissues of the distal limb elements can be afflicted by laminitis, pododermatitis, coronary band abscesses (Fowler and Miller, 2003); chronic foot disease (von Houwald and Flach, 1998); ulcerification and deep fissuring of the soft foot pad following penetrative trauma or unfavorable conditions underfoot (Jones, 1979; von Houwald and Guldenschuh, 2002); nails cracking (Jones, 1979; von Houwald and Guldenschuh, 2002); interdigital granulomas and papillomas (Jones, 1979; Fowler and Miller, 2003). In other ungulates, such as Hartmann's mountain zebra and the Patagonian huemul, hoof can undergrow pathological overgrowth, associated with unsuitable enclosure surfaces, genetic factors and copper-deficiency (Yates et al. (2004)) or other infective conditions (Flueck and Smith-Flueck, 2008). *Treponema*-induced infections in the hooves have been observed in the Wild Elk (Wilson-Welder et al., 2022), while severe pathological conditions (asymmetrical, markedly elongated, and curved or broken) in the same bones were observed in Roosevelt Elks (Han and Mansfield, 2014). Osteoarthritis was the most common reported bone pathology in rhinoceroses (Stilson et al., 2016), while other conditions were considered rare due to their intrinsic difficulties in recognizing their presence from an external observations, and to diagnose and to treat them in time. From this lack of knowledge, Regnault et al. (2013) analyzed bones from different White and Sumatran rhinoceroses (*Ceratotherium simum* and *Dicerorhinus sumatrensis*), reporting enthesophyte formation, osteoarthritis, remodelling (i.e., widening of normal cavities and cavernous excavation of the palmar or plantar bone), osteitis-osteomyelitis, fracture, and subluxation. Galateanu et al. (2013) also reported cortical sclerosis, proliferative new bone formation and remodelling, bony fragments, fractures, periosteal proliferation, osteolysis, bone rarefaction, and, in less frequency, bone cystic formation and ankylosis. Rhinocerotidae shows a long fossil

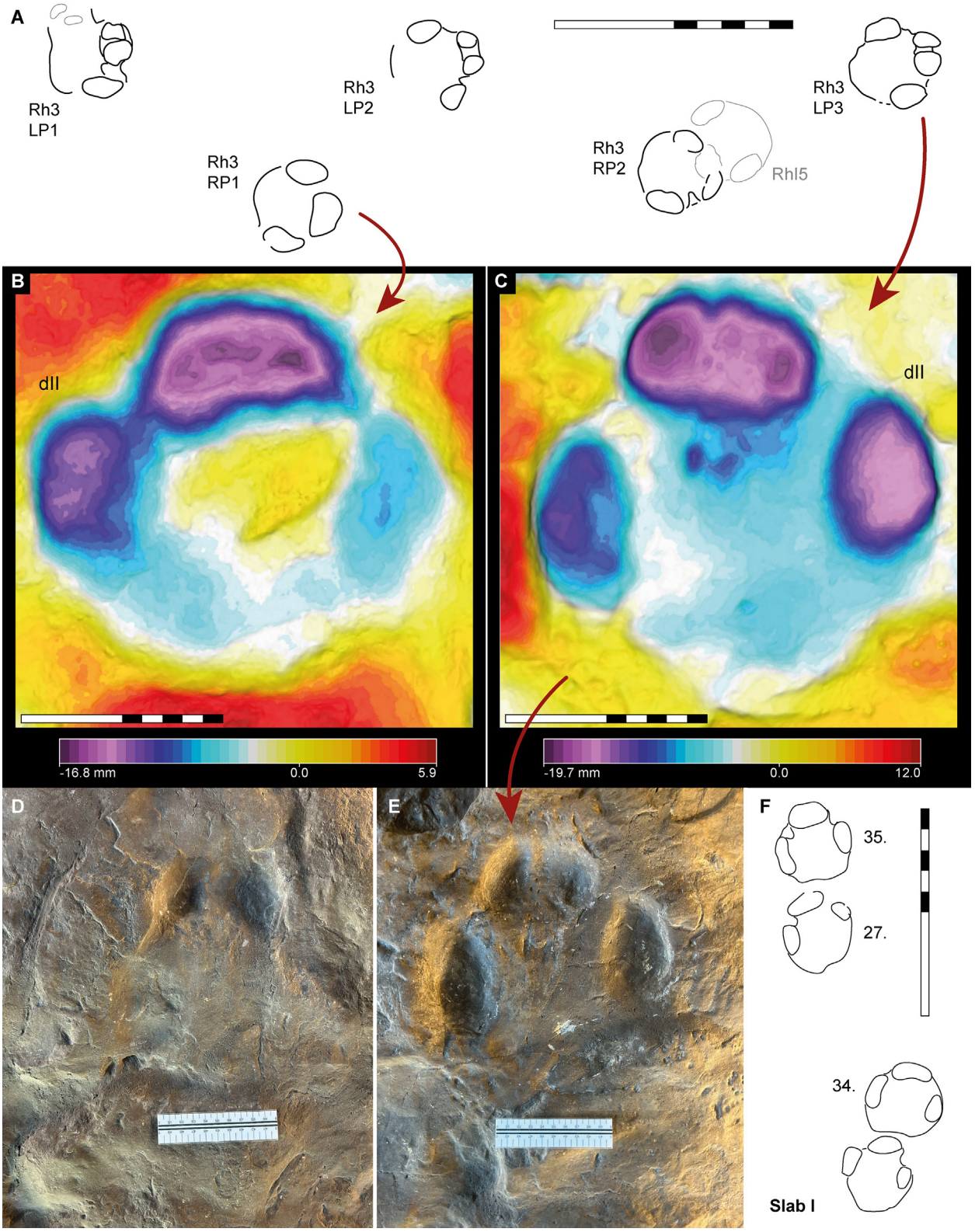

Fig. 4. Details of trackway Rh3. **A.** Outline drawings of the trackway. **B.** False-colour depth map of the normal track Rh3-RP1. **C.** False-colour depth map of malformed track Rh3-LP3, showing a clear bilobated split hoof of digit III. **D.** Photograph of Rh-LP2. While track is quite shallow, the impression of the bilobated digit III is quite clear. **E.** Photograph of Rh-LP3 with all digits and the atypical digit III hoof impressions well marked. **F.** Detail of the neotype trackway of *Rhinoceripeda tasnadyi* (Slab I, in the mezzanine corridor of the Hungarian Geological Institute; specimen V 2024.9.1) as defined by Kordos (1985). Tracks were outlined from the 3D models made by the authors and labelled accordingly to Kordos (1985: text-fig. 51). Scale bars: 50 cm (A, F), 10 cm (B-E).

record, spreading from the late Eocene (*Trigonias osborni*) up to Present days, with numerous limb and autopodium elements discovered (Stilson et al., 2016: table 2). Stilson et al. (2016) compared these materials in order to understand the possible presence of pathological patterns and distributions in the rhinocerotid limbs, and they observed how paleopathological occurrence, mostly referable to arthritic conditions, increases in younger taxa, being rarer in Eocene-Miocene species. Rhinocerotid taxa increased their body mass throughout their evolutionary history, and the authors identify a possible significant correlation of pathology with mass. Longevity might be another factor influencing this trend, as bigger animals can live longer, increasing the likelihood to suffer pathological conditions (Stilson et al., 2016).

Usually, zoo or captive populations tend to show more pathological conditions than wild population (Huchzermeyer, 2002), but even in these conditions the split of the central hoof as occurring in Rh3 is yet to be found and described, either in existing rhinocerotid individuals or in the fossil record of the clade.

5.3. MN4 Rhinocerotidae in Europe and the possible Ipolytarnóc trackmaker

Unfortunately, no cranial or postcranial remains have been collected form the study area. The diversity of Rhinocerotidae from MN4 is particularly high in Europe, as this mammal zone also testified the faunal renewal in Rhinocerotidae-assemblages with the disappearing of endemic species and of the last Oligocene taxa, and the arrival of new species from the East (Antoine et al., 2000; Antoine and Becker, 2013; Becker and Tissier, 2020). The genus *Plesiaceratherium* (or *Dromoceratherium*) is testified by three relatively slender species: *P. platyodon*, *P. lumiarense*, and *P. mirallesi*, the latter having an estimated body mass of 1200 kg and a gracility index of 0.26. The small and slender *Protaceratherium minutum* survives to the base of MN4 since the Oligocene, being reported in the French site of Artenay and Béon 2 (Antoine et al., 2000), while *Lartetotherium sansaniense* arrives for the first time in Europe during MN4b together with the large-sized teleoceratine *Brachypotherium* (body mass over 2000 kg) (Heissig, 2012). The species *Diaceratherium aurelianense* is typical of MN4a of Europe (Becker et al., 2009) while *D.* cf. *aurelianense* is reported at Eggingen-Mittelhart (Bayern, Germany), MN4b in age. This species has an estimated body mass of 1500 kg and a gracility index higher (0.30) than in *Plesiaceratherium*. The presence of the relatively small-sized elasmotheriine *Hispanotherium* (estimated body mass less than 1000 kg) also characterizes the MN4 zone, with *H. corcolense* and *H. beonense* occurring during MN4a and *H. beonense* and *H. matritense* during MN4b and MN5 (Antoine et al., 2002; Becker and Tissier, 2020). Considering the estimated body masses of the different taxa and the dimensions and proportions of the tracks, an attribution to a large size and graviportal rhinoceros, such as *Diaceratherium* or *Brachypotherium*, cannot be ruled out. However, a revision of the whole collection of tracks, and the estimation of the shoulder-height need to be performed to support any hypothesis.

6. Conclusions

Trackway Rh3 of the "Auditorium slab" (specimen Ob.1512) shows some peculiar pathology at the ungual of digit III of left pes, that is split in two. This is the first and so far unique case in the ichnological record, not only for Miocene rhinocerotid, but in general for this clade. This finding rises its importance considering that Eocene and Miocene rhinocerotids seems to show less malformations than modern ones (Stilson et al., 2016) and by the fact that similar malformation are unknown (or not published) also in modern rhinoceros.

Due to its rarity and the lack of comparison with modern examples, the precise cause of the malformation of hoof cannot be determined. It could have been a trauma, a disease or a developmental failure. Our measurements showed no clear gait variation, meaning that the animal was not heavily limping. This can be due to two causes: (*i*) whatever caused the malformation (trauma or disease), it happened long before the impression of the trackway, leaving the animal the time to adapt and compensate for the split hoof; (*ii*) our data, consisting only in 5 consecutive tracks, are incomplete; in this case the only solution to solve the issue would be to find the exact collection point, hoping more tracks of Rh3 are preserved to enlarge the dataset.

This last point opens to a wider reflection on how to recognise and assess (paleo)pathologies from the ichnological record. In this case, it was possible to spot the anomaly because the tracks belong to a trackway and are not isolated, and because of the huge reference dataset, including thousands of other tracks belonging to the same ichnotaxon and coming from the same locality and paleoenvironment, representing a wide set of variations due to different substrate or locomotion conditions (Falkingham, 2014). But what if there isn't a huge comparison record? In that case, either the pathology is clear (e.g., a missing digit in only one of the autopodium) or it can't be surely assessed. In an extreme situation, a trackway with some pathology could even become a type specimen for a new ichnotaxon, if not other reference material exists, causing issues in evaluating the diversity of an ichnocoenosis. We suggest here that more attention should be given to the occurrence of possible pathologies in the track record, especially in taxonomy-oriented studied.

Credit authorship contribution statement

M. Belvedere: Writing – review & editing, Writing – original draft, Visualization, Software, Methodology, Investigation, Formal analysis, Data curation, Conceptualization, Data acquisition. **F. Bertozzo:** Writing – review & editing, Writing – original draft, Methodology, Investigation, Conceptualization. **G. Botfalvai:** Writing – review & editing, Writing – original draft, Visualization, Resources, Investigation, Conceptualization. **L. Pandolfi:** Writing – review & editing, Writing – original draft, Investigation, Funding acquisition, Formal analysis, Conceptualization, Data acquisition.

Data availability

Data will be made available on request.

Declaration of competing interest

The authors declare that they have no known competing financial interests or personal relationships that could have appeared to influence the work reported in this paper.

Acknowledgements

We thank M. Gasparik (Hungarian Natural History Museum), L. Makádi (Supervisory Authority for Regulatory Affairs, former Mining and Geological Survey of Hungary), I. Szarvas and T. Juhász (Ipolytarnóc Fossils Nature Conservation Area of the Bükk National Park) for providing access to the type specimen and locality of *Rhinoceripeda tasnadyi*. LP received support from Synthesys+ (access to HU-TAF) and operated under the recognition of the Ministry of Foreign Affairs and International Cooperation (DGDP UFF.VI, n. 1444, n. 2806) for part of this research. The research was supported

by the SKHU/1902/1.1/037 INTERREG project of the Bükk National Park Directorate and HUN-REN Hungarian Research Network (GB). We thank two reviewers whose comments strongly improved the manuscript. This is HUN-REN-MTM-ELTE Paleo contribution No. 402.

Appendix A. Supplementary material

Supplementary data to this article can be found online at https://doi.org/10.1016/j.geobios.2024.08.009.

References

Antoine, P.-O., Alférez, F., Iñigo, C., 2002. A new elasmotheriine (Mammalia, Rhinocerotidae) from the Early Miocene of Spain. Comptes Rendus Palevol 1, 19–26.

Antoine, P.-O., Becker, D., 2013. A brief review of Agenian rhinocerotids in Western Europe. Swiss Journal of Geosciences 106, 135–146.

Antoine, P.-O., Bulot, C., Ginsburg, L., 2000. Les rhinocérotidés (Mammalia, Perissodactyla) de l'Orléanien (Miocène inférieur) des bassins de la Garonne et de la Loire : intérêt biostratigraphique. Comptes Rendus de l'Académie des Sciences, Sciences de la Terre et des Planètes, Paris 330, 571–576.

Avanzini, M., Pinuela, L., Garcia-Ramos, J., 2008. Theropod palaeopathology inferred from a Late Jurassic trackway, Asturias (N. Spain). Oryctos 8, 71–75.

Bartkó, L., 1985. Geology of Ipolytarnóc. Geologica Hungarica, Series Palaeontologica 44, 49–71.

Becker, D., Bürgin, T., Oberli, U., Scherler, L., 2009. A juvenile skull of *Diceratherium lemanense* (Rhinocerotidae) from the Aquitanian of Eschenbach (eastern Switzerland). Neues Jahrbuch für Geologie und Paläontologie Abhandlungen 254, 5–39.

Becker, D., Tissier, J., 2020. Rhinocerotidae from the early middle Miocene locality Gračanica (Bugojno Basin, Bosnia-Herzegovina). Palaeobiodiversity and Palaeoenvironments 100, 395–412.

Belvedere, M., Fabre, E., Pandolfi, L., Legal, S., Coster, P., 2023. Stepping into Oligocene. A reassessment of the early Oligocene mammal tracks from Saignon (SE France). Historical Biology, 1–17. https://doi.org/10.1080/08912963.2023.2286275.

Böckh, H., 1902. Report of the director. Magyar Királyi Földtani Intézet Jelentése 1900-ról., 33-34.

Botfalvai, G., Magyar, J., Watah, V., Szarvas, I., Szolyák, P., 2022. Large-sized pentadactyl carnivore footprints from the early Miocene fossil track site at Ipolytarnóc (Hungary): 3D data presentation and ichnotaxonomical revision. Historical Biology 35, 1709–1725.

Csepreghyné, M.I., 1967. Az Ipolytarnoci Burdigalai fauna. Földtani Közlöny 97, 177–185.

Dantas, P., dos Santos, V., Lockley, M., Meyer, C., 1994. Footprint evidence for limping dinosaurs from the Upper Jurassic of Portugal. Gaia 10, 43–48.

Falkingham, P.L., 2014. Interpreting ecology and behaviour from the vertebrate fossil track record. Journal of Zoology 292, 222–228.

Falkingham, P.L., Bates, K.T., Avanzini, M., Bennett, M., Bordy, E.M., Breithaupt, B.H., Castanera, D., Citton, P., Díaz-Martínez, I., Farlow, J.O., Fiorillo, A.R., Gatesy, S.M., Getty, P., Hatala, K.G., Hornung, J.J., Hyatt, J.A., Klein, H., Lallensack, J.N., Martin, A.J., Marty, D., Matthews, N.A., Meyer, C.A., Milàn, J., Minter, N.J., Razzolini, N.L., Romilio, A., Salisbury, S.W., Sciscio, L., Tanaka, I., Wiseman, A.L.A., Xing, L.D., Belvedere, M., 2018. A standard protocol for documenting modern and fossil ichnological data. Palaeontology 61, 469–480.

Flueck, W.T., Smith-Flueck, J.A.M., 2008. Age-independent osteopathology in skeletons of a South American cervid, the Patagonian huemul *(Hippocamelus bisulcus*). Journal of Wildlife Diseases 44, 636–648.

Fowler, M.E., Miller, R.E., 2003. Zoo and Wild Animal Medicine. Saunders, St. Louis, Missouri.

Galateanu, G., Hildebrandt, T.B., Maillot, A., Etienne, P., Potier, R., Mulot, B., Saragusty, J., Hermes, R., 2013. One small step for rhinos, one giant leap for wildlife management-imaging diagnosis of bone pathology in distal limb. PLoS One 8, e68493.

Gradstein, F.M., Ogg, J.G., Schmitz, M., 2012. The Geological Time Scale 2012. Elsevier Science, Oxford.

Hably, L., 1985. Early Miocene plantfossils from Ipolytarnóc, N Hungary. Geologica Hungarica, Series Geologica 45, 73–255.

Han, S., Mansfield, K.G., 2014. Severe hoof disease in free-ranging Roosevelt elk (*Cervus elaphus roosevelti*) in southwestern Washington, USA. Journal of wildlife diseases 50, 259–270.

Harangi, S.z., 2001. Neogene to Quaternary volcanism of the Carpathian-Pannonian Region – a review. Acta Geologica Hungarica 44, 223–258.

Heissig, K., 2012. Les Rhinocerotidae (Perissodactyla) de Sansan. Mémoires du Muséum national d'Histoire naturelle de Paris 203, 317–485.

Huchzermeyer, F.W., 2002. Diseases of farmed crocodiles and ostriches. Revue scientifique et technique-Office international des épizooties 21, 265–276.

Ishigaki, S., Lockley, M.G., 2010. Didactyl, tridactyl and tetradactyl theropod trackways from the Lower Jurassic of Morocco: evidence of limping, labouring and other irregular gaits. Historical Biology 22, 100–108.

Jones, D., 1979. The husbandry and veterinary care of captive rhinoceroses. International Zoo Yearbook 19, 239–250.

Kanniappan, S., Gopinadhan, A., 2024. Functional recovery of a spotted deer (axis axis) from unilateral multiple limb compound fractures with management of capture myopathy syndrome: a case report. Journal of Current Veterinary Research 6, 246–252.

Karátson, D., Biró, T., Portnyagin, M., Kiss, B., Paquette, J.L., Cseri, Z., Hencz, M., Németh, K., Lahitte, P., Márton, E., Kordos, L., Józsa, S., Hably, L., Müller, S., Szarvas, I., 2022. Large-magnitude (VEI $\geq$ 7) 'wet' explosive silicic eruption preserved a Lower Miocene habitat at the Ipolytarnóc Fossil Site, North Hungary. Scientific Reports 12, 9743.

Kocsis, L., 2007. Centralparatethyan shark fauna (Ipolytarnóc, Hungary). Geologica Carpathica-Bratislava 58, 27–40.

Kocsis, L., Vennemann, T.W., Hegner, E., Fontignie, D., Tütken, T., 2009. Constraints on Miocene oceanography and climate in the Western and Central Paratethys: O-, Sr-, and Nd-isotope compositions of marine fish and mammal remains. Palaeogeography, Palaeoclimatology, Palaeoecology 271, 117–129.

Kordos, L., 1985. Footprints in the Lower Miocene sandstone of Ipolytarnóc. Geologica Hungarica, Series Geologica 46, 257–415.

Lallensack, J.N., Buchwitz, M., Romilio, A., 2022. Photogrammetry in ichnology: 3D model generation, visualisation and data extraction. Journal of Paleontological Techniques 22, 1–18.

Lukács, R., Guillong, M., Bachmann, O., Fodor, L., Harangi, S.z., 2021. Tephrostratigraphy and magma evolution based on combined zircon trace element and U-Pb age data: fingerprinting Miocene silicic pyroclastic rocks in the Pannonian basin. Frontiers in Earth Science 9, 615768.

Lukács, R., Harangi, S.z., Gál, P., Szepesi, J., Di Capua, A., Norini, G., Sulpizio, R., Groppelli, G., Fodor, L., 2022. Formal definition and description of lithostratigraphic units related to the Miocene silicic pyroclastic rocks outcropping in Northern Hungary: a revision. Geologica Carpathica 73, 137–158.

Mallison, H., Wings, O., 2014. Photogrammetry in paleontology – A practical guide. Journal of Paleontological Techniques 12, 1–31.

Marchetti, L., Belvedere, M., Voigt, S., Klein, H., Castanera, D., Díaz-Martínez, I., Marty, D., Xing, L., Feola, S., Melchor, R.N., Farlow, J.O., 2019. Defining the morphological quality of fossil footprints. Problems and principles of preservation in tetrapod ichnology with examples from the Palaeozoic to the present. Earth-Science Reviews 193, 109–145.

Márton, E., Vass, D., Tunyi, I., Marton, P., Zelenka, T., 2007. Paleomagnetic properties of the ignimbrites from the famous fossil footprints site, Ipolytarnóc (close to the Hungarian-Slovak frontier) and their age assignment. Geologica Carpathica 58, 531.

Matthews, N., Noble, T., Breithupt, B.H., 2016. Close-Range photogrammetry for 3D ichnology: the basics of photogrammetric ichnology. In: Falkingham, P.L., Marty, D., Richter, A. (Eds.), Dinosaur tracks – the next steps. Indiana University Press, Bloomington and Idianapolis, pp. 28–55.

McCrea, R., Buckley, L., Farlow, J., Lockley, M., Currie, P., Matthews, N., Pemberton, G., 2014. A "Terror of *Tyrannosaurs*": the first trackways of Tyrannosaurids and evidence of gregariousness and pathology in Tyrannosauridae. PLoS ONE 9, e103613.

McCrea, R., Tanke, D., Buckley, L., Lockley, M., Farlow, J., Xing, L., Matthews, N., Helm, C., Pemberton, S., Breithaupt, B., 2015. Vertebrate ichnopathology: pathologies inferred from dinosaur tracks and trackways from the mesozoic. Ichnos 22, 235–260.

Oliva, C., Arregui, M., 2018. Mammalian Ichnopathology: a case study of Holartic Ungulates (Gomphotheriidae, Equidae, Camelidae) of the Late Pleistocene of South America. Ichnotaxomic implications. Boletín de la Sociedad Geológica Mexicana 70, 417–447.

Pálfy, J., Mundil, R., Renne, P.R., Bernor, R.L., Kordos, L., Gasparik, M., 2007. U-Pb and $^{40}Ar/^{39}Ar$ dating of the Miocene fossil track site at Ipolytarnóc (Hungary) and its implications. Earth and Planetary Science Letters 258, 160–174.

Paratte, G., Lapaire, M., Lovis, C., Marty, D., 2018. Contexte et méthode. Office de la culture, Paléontologie A16, Porrentruy.

Piller, W.E., Harzhauser, M., Mandic, O., 2007. Miocene Central Paratethys stratigraphy – current status and future directions. Stratigraphy 4, 151–168.

Regnault, S., Hermes, R., Hildebrandt, T., Hutchinson, J., Weller, R., 2013. Osteopathology in the feet of rhinoceroses: lesion type and distribution. Journal of Zoo and Wildlife Medicine 44, 918–927.

Rögl, F., 1998. Palaeogeographic considerations for Mediterranean and Paratethys seaways (Oligocene to Miocene). Annalen des Naturhistorischen Museums in Wien 99A, 279–310.

Stilson, K.T., Hopkins, S.S., Davis, E.B., 2016. Osteopathology in Rhinocerotidae from 50 million years to the present. PLoS One 11, e0146221.

Sztanó, O., 1994. The tide-influenced Pétervására sandstone, early Miocene, Northern Hungary: sedimentology, palaeogeography and basindevelopment. Geologica Ultraiectina 120, 1–155.

Tasnádi Kubacska, A., 1976. Traces of Prehistoric Life in the Sandstone with Footprints at Ipolytarnóc Village (N Hungary). Annual Report of the Geological Institute of Hungary 1976, 77–94.

Vialov, O.S., 1965. Stratigrafiya Neogenovykh molass Predkarpatskovo progriba [Stratigraphy of the Neogene molasse of the PreCarpathian basin]. Naukova

Dumka (Akademiya Nauk Ukrainskoy SSR Institut Geologii I Geokhimii Goryuchikh Iskopayemykh), Kiev.

von Houwald, F., Flach, E., 1998. Prevalence of chronic foot disease in captive greater one-horned rhinoceros (*Rhinoceros unicornis*). European Association of Zoo and Wildlife Veterinarians Scientific Meeting 2, 323–327.

von Houwald, F., Guldenschuh, G., 2002. Husbandry Manual for the Greater One-Horned or Indian Rhinoceros (*Rhinoceros unicornis*) Linné, 1758. Basel Zoo, Basel, Switzerland.

Wilson-Welder, J.H., Mansfield, K., Han, S., Bayles, D.O., Alt, D.P., Olsen, S.C., 2022. Lesion material from treponema-associated hoof disease of wild Elk induces disease pathology in the sheep digital dermatitis model. Frontiers in Veterinary Science 8, 782149.

Yates, K., Plowman, A., Macdonald, C., 2004. Hoof overgrowth in Hartmann's mountain zebra is a consequence of diet, substrate, and behaviour. In: Proceedings of the 6th Annual Symposium on Zoo Research. Edinburgh Zoo, Edinburgh, UK, pp. 305–312.